Classification: Biological Sciences, Population Biology

The risk of Type 2 oral polio vaccine use in post-cessation outbreak response

Kevin A. McCarthy*[1], Guillaume Chabot-Couture[1], Michael Famulare[1], Hil M. Lyons[1], Laina D. Mercer[1]

[1]Institute for Disease Modeling, Bellevue, WA, USA

*Corresponding author: +1-425-247-2145, kmccarthy@idmod.org

Keywords: Poliovirus, Eradication, oral polio vaccine

Abstract

Wild type two poliovirus (WPV2) was last observed in 1999. The Sabin-strain oral polio vaccine type two (OPV2) was critical to eradication, but is known to revert to a neurovirulent phenotype, causing vaccine-associated paralytic poliomyelitis (VAPP). OPV2 is also transmissible and can establish circulating lineages, called circulating vaccine-derived polioviruses (cVDPVs), which can also cause paralytic outbreaks. Thus, in April 2016, OPV2 was removed from immunization activities worldwide. Interrupting transmission of cVDPV2 lineages that survive cessation will require OPV2 in outbreak response, which risks seeding new cVDPVs; this potential cascade of outbreak responses seeding new vaccine-derived lineages, thus necessitating further outbreak responses, presents a critical risk to the polio eradication effort.

The EMOD individual-based disease transmission model was used to investigate the risk of cVDPV2 establishment following OPV2 use in outbreak response in West African populations**.** Under a broad range of scenarios, the probability that OPV2 use in outbreak response establishes new cVDPV2 lineages in this model exceeds 50% in as little as 18 months and no later than four years post-cessation. The risk of a cycle in which outbreak responses seed new cVDPV2 lineages suggests that OPV2 use should be managed carefully as time from cessation increases. Key approaches to mitigating the risk that OPV2 use will be needed in the far future focus on extinguishing existing cVDPV2 lineages soon: maintaining high-quality surveillance, conducting aggressive near-term outbreak responses, strengthening IPV in routine immunization, and gaining access to currently inaccessible areas of the world to conduct surveillance.

Significance Statement

Wild type two poliovirus (WPV2) was last observed in 1999, and the type 2 oral polio vaccine (OPV2) was a critical tool in eradication. However, OPV2 is a live attenuated virus, which is able to spread in human populations and regain neurovirulence (becoming circulating vaccine-derived poliovirus, or cVDPV). Ending the use of OPV2 is therefore critical to global poliovirus eradication, and in April 2016, OPV2 was removed from immunization activities worldwide. However, interrupting transmission of any extant cVDPVs will require local use of OPV2, which risks seeding new cVDPVs; the potential for this cycle presents a critical risk to the polio eradication effort. This work investigates the conditions under which OPV2 immunization activities risk seeding new cVDPV lineages.

Background

April 2016 marks the global cessation of the use of the Sabin-strain oral polio vaccine type two (OPV2) in routine and campaign immunization, with all 155 OPV-using countries switching from the trivalent to the bivalent form of OPV, which contains only vaccine types 1 and 3 (1). The last case of wild type 2 poliovirus (WPV2) was observed in India, in 1999 (2). OPV2 is a live, attenuated virus, capable of genetic reversion to a neurovirulent phenotype that imposes a health burden due to vaccine-associated paralytic polio (VAPP). The Sabin-strain viruses are also capable of transmission, and in low-immunity settings can establish circulation; these established lineages are termed circulating vaccine-derived polioviruses (cVDPVs) (3–6). Among the three OPV serotypes, OPV2 is estimated to cause 40% of all VAPP cases, and 90% of all cVDPV cases (7). The successful removal of OPV2 from elective use therefore presents clear public health benefits. However, the cessation of OPV2 immunization carries the implicit risk that Sabin-strain lineages will survive to become cVDPV2s in the future, necessitating outbreak response with OPV2, thereby potentially seeding new lineages (8, 9). Historical experience has established that Sabin-strain polioviruses (and other live, attenuated polioviruses) are able to broadly circulate within populations when introduced after relatively brief (1-3 year) interruptions in OPV use (10–13). The possibility of a cycle in which OPV2 use in outbreak response seeds new cVDPV2 lineages, necessitating further outbreak response, represents a fundamental risk to the cessation of OPV2 immunization.

This manuscript addresses the conditions under which OPV2 use in outbreak response could establish new chains of Sabin 2 transmission, and how this risk evolves as population immunity declines post-cessation. Many factors affect an outbreak response activity's propensity to establish new VDPV2 lineages: population immunity at the time of outbreak response, the base reproductive rate R_0 of the Sabin type 2 virus (which may change during genetic reversion), and the epidemiological connectedness of spatially separated populations. Each of these factors is also highly uncertain, and varies with the geographical/societal context under consideration. In this work, a variety of potential scenarios are considered (see Table 1: Description of parameters varied across simulated scenarios.Table 1), and in each scenario, a Separatrix algorithm (14). is used to quantify the risk that an outbreak response conducted according to existing protocol will seed a new VDPV2 as a function of the time since cessation and the mean per-person per-day migration rate between provinces.

Table 1: Description of parameters varied across simulated scenarios.

Quantity varied	Values
Final base reproductive rate of reverted VDPV2 (R_{0f})	{1·2, 1·5, 2·0, 3·0}
Initial reproductive rate of OPV2 as fraction of final R_0 (f)	{0·25, 0·5}
Exponential timescale of R_0 reversion (λ)	{60 days, 150 days}
# of IPV doses given to children born after OPV2 cessation (N_{IPV})	{0, 1}
Distance-dependence of migration rates (c)	{-1, -2} (1/d, $1/d^2$)
Population immunity in cohort of children born before OPV2 cessation	Induced by three OPV campaigns at 80% coverage and 50% take (moderate immunity), or three OPV campaigns at 100% coverage and 100% take (high immunity)

Results

Figure 1 presents the output of a single run of the Separatrix algorithm, with R_{0f} = 2·0, f = 0·5, λ= 60 days, N_{IPV}= 1, c= 1 (see Table 1 for definition of symbols). Figures 1-3 all present comparisons at the moderate immunity profile (defined in Table 1) in the pre-cessation birth cohort. The color surface shows the imputed risk throughout a 2D space of mean migration rate and time since cessation; the gray crosses and circles indicate simulations in which a new lineage succeeds or fails, respectively, to establish long-term circulation (defined for the purposes of this study as continued viral transmission, outside of the response provinces, 9 months after the outbreak response); the thin black dashed box outlines a space of migration rates preferred by a calibration to a previous travelling outbreak of WPV1 in the region (Supplement); and the black line represents the 50% separatrix line, the imputed contour in parameter space along which the VDPV2 risk is 50%. In this scenario, this line indicates that this risk reaches 50% around 2·5-3·5 years post-cessation, depending on the migration rate.

Scenario comparison –dependence of VDPV2 risk on infectivity profile

It is difficult to visually compare the full risk surfaces of multiple scenarios, so the 50% separatrix contours derived in different scenarios are used to compare the relative risks. Figure 2 illustrates how the risk profile depends on R_{0f} and f, with other parameters held constant (λ= 60 days, N_{IPV}= 1, c= 1). As expected, the risk of continued circulation rises earlier with increasing R_0 of fully reverted OPV2; the lowest tested value, 1·2, presents minimal risk even five years post-cessation in the preferred migration rate region, while the highest value, 3·0, presents high risk just 18 months post-cessation. At a given R_{0f}, changing f from 0·5 to 0·25 induces a small but non-negligible shift of the separatrix to later times/higher migration rates.

Scenario comparison – dependence of VDPV2 risk on IPV use in routine immunization post-cessation

Figure 3 illustrates how the inclusion of IPV in routine immunization (RI) affects the risk of OPV2 survival in this model. The coverage of routine immunization is assumed to be 80%. While the herd immunity effects of IPV are evident in developed nations, where the oral-oral transmission route likely dominates (15, 16). they are poorly characterized in developing countries where the fecal-oral transmission route dominates. At the individual level, recent mOPV2 challenge studies comparing a variety of mixed IPV-bOPV schedules have found that mixed IPV-bOPV schedules provide heterotypic mucosal immunity to Type 2 that appears superior to bOPV or IPV alone but inferior to mOPV2 or tOPV (17, 18). It is not immediately apparent from literature whether additional IPV doses beyond the first induce a dose-dependent increase in this heterotypic immunity, or whether this incremental effect depends on the ordering of bOPV and IPV in the schedule (17, 18). The observed induced immunity reduces both the probability of acquisition upon mOPV2 challenge and the duration and amount of Sabin 2 shedding in stool. At the population scale, it is unclear how this reduction in acquisition at challenge doses translates to protection at natural exposure levels, and how the reduction in shedding translates to reduced infectiousness in close-contact and community settings in regions of poor sanitation (19, 20). In this model, it is assumed that children born post-cessation will be bOPV-exposed, and that a dose of IPV in RI will confer some degree of heterotypic protection – a 10% reduction in the recipient's effective exposure and a 10% reduction in a recipient's onward infectivity are assumed; given the uncertainties around incremental effects of additional doses, a 2xIPV RI schedule is not compared here. In the model, the IPV distributed during outbreak response will have similar effects on the OPV2-naïve, but induce a boosting response in the OPV2-exposed. Under these assumptions about bOPV+IPV immunization,

Figure 3 shows that even the limited mucosal protection that a dose of IPV in RI provides can substantially mitigate OPV2 survival if the reverted Sabin $R_{0,f}$ is low, but this mitigating effect declines as $R_{0,f}$ increases.

Scenario comparison – dependence of VDPV2 risk on immunity profile at OPV2 cessation

Finally, Figure 4 presents a comparison of the two potential pictures of immunity at the time of cessation. The solid lines indicate simulations with pre-cessation population immunity in zero-to-five year olds induced by three OPV campaigns at 80% coverage, 50% take; the dashed lines indicate sims with 100% coverage, 100% take (essentially, perfect immunity within this cohort). The dashed lines essentially indicate the time at which the cohort of children born after OPV2 cessation will be able to sustain circulation of OPV2 in the absence of any transmission through the older cohort. The duration of the additional protection from perfect pre-cessation immunity increases as $R_{0,f}$ increases, as the virus is increasingly able to recruit the partially immune older children into the transmission chain. The additional protection against cVDPV2 establishment provided by perfect immunity in the older cohort is modest given the extreme nature of this assumption, as the naïve cohort of children born post-cessation eventually grows sufficiently large to sustain transmission.

The other scenario parameters (the distance-dependence in the gravity model of migration, the reversion rate of OPV2 infectivity) are both found to have comparatively small effects on the position of the separatrix line; the figures illustrating the comparisons between these scenarios can be found in the supplemental materials.

Discussion

The population immunity conditions in the upcoming years will be unprecedented; little to no immunity will be acquired through natural infection as in the pre-vaccine era, and Type 2 immunity will be provided solely through IPV, with little ability to induce strong intestinal mucosal immunity. Any observed cVDPV2 must be extinguished, and OPV2 is the best currently available tool for doing so, but outbreak response activities post-cessation will infect a sizable population with the OPV2 virus in a world with an ever-growing young cohort lacking intestinal mucosal immunity. While uncertainty in immunity, transmission, and migration conditions prevent a strongly constrained estimate of this risk vs. time in a particular context, the results of this study indicate that under a wide range of conditions, outbreak responses as currently outlined could potentially create a cascade of new outbreaks within 18 months to four years post-cessation.

Once population immunity becomes low enough to support circulation, it is unclear whether this risk can be mitigated without new vaccines that induce mucosal immunity without transmitting efficiently or reverting to neurovirulence. In the near-term, minimizing the risk of cascading cVDPV2 outbreaks requires strategies that minimize the risk that OPV2 use will be required at all in the future.

1. **Strengthen both paralysis-based and environmental poliovirus surveillance.** In the absence of OPV2 use, the emergence of cVDPV2 relies on the unobserved survival of lineages seeded before cessation. Detecting and interrupting any cVDPV2 lineages currently circulating, while global population immunity is high, minimizes the risk of cascading cVDPV2 outbreaks in the future. Environmental surveillance provides the ability to detect poliovirus in a population in

the absence of paralytic cases, and could be used to track Sabin 2 survival in the near-term to identify places of concern early.

2. **Aggressive outbreak response in the near-term.** The emergence of VDPV2 in the near-term will be an effective indicator of locally low population immunity in a world in which immunity remains high. Near-term OPV2 use does not present substantially more risk than did its use immediately pre-cessation. Widespread cVDPV2 circulation has been observed in the past (21, 22), and immunity conditions post-cessation will be unprecedented due to a lack of both natural and vaccine-derived immunity. These facts argue for outbreak responses soon after cessation to be geographically broad, both to ensure interruption of the observed transmission chain and to raise population immunity in regions surrounding the emergence. It may be advantageous to heighten surveillance in neighboring districts or countries known to have imported polioviruses in the past from the emergence region.
3. **IPV in routine immunization**. Under the (admittedly uncertain) assumptions about IPV-induced intestinal mucosal immunity used in this study, high-coverage IPV immunization in RI could mitigate the OPV2 survival risk for a short time. Even if these results overestimate the herd effect of cross-protection from bOPV+IPV exposure in the post-cessation cohort, scaling up the coverage and number of doses of IPV in RI would provide valuable individual protection against paralysis, reducing the burden of VDPV2 outbreaks or VAPP caused by OPV2 response.
4. **IPV in immunization campaigns**. A second crucial feature of IPV in the post-cessation world is its ability to boost mucosal immunity against Type 2 in OPV2-exposed children. While the use of IPV in outbreak response campaigns is already a piece of the outbreak response protocol, IPV immunization campaigns targeting both the pre- and post-cessation cohort of children could serve two purposes. First, filling gaps in routine immunization, which are quite large in much of the developing world. Second, boosting Type 2 immunity in the older, OPV2-exposed cohort. This work has not addressed the question of waning mucosal immunity, but if mucosal immunity wanes on relatively short timescales, this waning could be counteracted through IPV boosting.
5. **Obtain access to currently inaccessible areas**. Regions of the world that are currently inaccessible to effective surveillance or outbreak response due to violence, instability, or local resistance, present significant risks where VDPV2 lineages could circulate unobserved. In Borno state, Nigeria, many areas have been inaccessible for years due to Boko Haram activity. In this state, both cVDPV2 (environmental isolation March 2016, most recent observed relative from May 2014) and WPV1 (paralysis onsets in July 2016, most recent observed relatives from 2011) have been recently observed.(23, 24) These discoveries highlight the critical risk that inaccessible areas present the polio eradication and OPV cessation efforts.

Most of these items are already priorities of the Global Polio Eradication Initiative, and the idea that OPV use in a post-cessation world presents a risk of seeding new cVDPVs is not new (9). The results of this study emphasize the immediacy of this risk, highlighting that the “honeymoon period”, during which the risks associated with OPV2 use remain low, is transient and could be quite brief. Near-term cVDPV2 outbreak responses must therefore serve the dual purposes of interrupting an observed chain of transmission and preventing the emergence of new ones, and all tools available should be applied

during this honeymoon period to minimizing the chances that OPV2 use in outbreak response will become necessary in 2018 or beyond.

In the long-term, in the event that all VDPV2 lineages are extinguished, the polio-free world will remain at risk of reintroduction from accidental release of VDPV2, bioterrorism, and long-term poliovirus shedding from immunocompromised individuals (25, 26). Preclinical development of stabilized, live attenuated polio vaccines, aiming to provide mucosal immunity with reduced risk of causing cVDPV, is underway (27–29). Successful development of such a tool would provide a safer tool for outbreak elimination and immunity maintenance in the post-cessation world.

In conclusion, as population immunity to Type 2 poliovirus transmission declines in upcoming years, the use of OPV2 in outbreak response will present an increasing risk of seeding new cVDPV2 lineages, putting the entire cessation effort at risk. While exact transmission conditions are uncertain and vary across geographic contexts, and the probability of observing new VDPV lineages from pre-cessation OPV use should decline over time, this risk may grow to alarming levels within as little as 18 months. Without new tools to induce strong mucosal immunity, it is unclear whether this risk can be mitigated in the long term. In the short-term, this potential outcome implies a need for strategies that minimize the risk that OPV2 use will be needed in the future: maintaining high-quality surveillance systems, broadening near-term outbreak responses, strengthening access to IPV in routine immunization, negotiating access to currently inaccessible areas. In the long-term, continuing the push for new polio vaccines that can induce mucosal immunity with reduced risks of transmission or reversion is important in the event of accidental or intentional Type 2 poliovirus release into a highly susceptible population.

Methods

Model specification

The generic disease branch of the individual-based disease modeling software EMOD DTK v2.8 was used to model polio transmission (30); a complete specification of the employed model can be found in the supplemental material. Transmission takes place on a network of populations representing Level One administrative divisions (provinces) throughout 16 countries in West Africa (details in Supplement). Within a province, disease transmission dynamics are governed by a susceptible-exposed-infectious-susceptible equation system with partial immunity, and transmission between the provinces proceeds through individual-level migration. As ~98% of all cVDPV2 paralysis cases in the AFRO region have arisen in the cohort of children under 5 years of age (polio paralysis data from POLIS) (31), the model tracks only infection and transmission in the under-5 cohort.

Modeling scenarios

For simplicity, initial population immunity is treated as constant across the provinces. The cohort of children old enough to have been alive at cessation is initialized with one of two immunity profiles: one consistent with having experienced three rounds of OPV2 distribution, at 80% population coverage (independent coverage per round) and 50% vaccine take, and one with three rounds at 100% coverage and take (an unrealistic assumption, but useful for comparison). The cohort born since cessation is assumed to be OPV2-naïve, but depending on the scenario, they may receive zero or one doses of the inactivated polio vaccine (IPV), which induces strong protection from paralysis (humoral immunity), little protection against acquisition and onward transmission (intestinal mucosal immunity) in OPV2-naïve

individuals, and a strong intestinal mucosal boosting response in OPV2-exposed individuals (details in Supplement) (17, 18, 20, 32, 33). No waning of immunity over time is modeled.

The survival of VDPV2 lineages from pre-cessation OPV2 use is not modeled here; it is simply assumed that an outbreak response has been triggered at a given time since cessation. The recent discovery in Borno State, Nigeria of cVDPV2 and WPV1 viruses from lineages unobserved for two and five years, respectively, demonstrates that prolonged unobserved circulation is feasible under suboptimal surveillance (8, 24, 34). In the model, an initial rapid-response OPV2 campaign targets Zamfara Province, Nigeria. Sixteen days later, an OPV2 campaign targets Zamfara and the bordering provinces Sokoto, Katsina, Kaduna, and Kebbi, followed by a joint OPV2\IPV campaign (taking advantage of IPV's mucosal boosting effect in OPV-exposed individuals) and a third OPV2 campaign in the same provinces at four-week intervals.

It is unclear how (or whether) the transmissibility of the OPV2 virus changes during genetic divergence from the Sabin strain. Here, the infectivity of Sabin 2 virus is assumed to be some fraction f of the fully-reverted infectivity, and to follow an exponential approach to a final infectivity (Supplement Eq. 2). The values of the initial and final infectivities, as well as the timescale of the exponential approach, are varied in the modeling scenarios.

Post-cessation simulations

A Separatrix algorithm (14) is used to explore the risk of OPV2 survival in the outbreak response described above, as a function of the time since cessation and the mean per-person per-day migration rate. A new circulating lineage is considered to have arisen whenever there are individuals infected with the virus, outside of the original response region, nine months after the outbreak response. The algorithm is terminated after only two rounds; a first round in which 500 samples are cast throughout the 2D space, and a second in which 500 additional points are targeted to map the contour in parameter space that produces a 50% probability of this outcome.

Availability of data and analysis code

The code developed for running the simulations and analyzing outputs is available at https://github.com/AMUG/OPV_PostCessation_Response_Project.

Simulation outputs and all non-confidential supporting data is available at https://www.dropbox.com/sh/vqk8878p1ch9oog/AACyBjP96-lh6qOOU_zgBIOCa?dl=0.

Permission for access to the Polio Information System (POLIS) case and campaign databases, and use of WHO shapefiles, was granted to the Institute for Disease Modeling researchers through the World Health Organization. The boundaries and names shown and the designations used in the maps in the supplement of this document do not imply the expression of any opinion whatsoever on the part of the World Health Organization concerning the legal status of any country, territory, city, or area or of its authorities, or concerning the delimitation of its frontiers or boundaries.

Acknowledgements
The authors would like to thank Steve Kroiss, Philip Eckhoff, and other colleagues at the Institute for Disease Modeling; Jay Wenger, Ananda Bandyopadhyay, and Arie Voorman at the Bill and Melinda Gates Foundation for critical feedback. This work was supported by Bill and Melinda Gates through the Global Good Fund.

References

1. World Health Organization (2016) Global switch in oral polio vaccines Situation report. Available at: http://web.archive.org/web/20160802181557/http://maps.who.int/OPV_switch/ [Accessed August 2, 2016].
2. World Health Organization (2015) Global eradication of wild poliovirus type 2 declared. Available at: https://web.archive.org/web/20160802182045/http://www.polioeradication.org/mediaroom/newsstories/Global-eradication-of-wild-poliovirus-type-2-verified/tabid/526/news/1289/Default.aspx [Accessed August 2, 2016].
3. Jenkins HE, et al. (2010) Implications of a circulating vaccine-derived poliovirus in Nigeria. *N Engl J Med* 362(25):2360–9.
4. Rakoto-Andrianarivelo M, et al. (2008) Reemergence of recombinant vaccine-derived poliovirus outbreak in Madagascar. *J Infect Dis* 197(10):1427–35.
5. Yang C-F, et al. (2003) Circulation of Endemic Type 2 Vaccine-Derived Poliovirus in Egypt from 1983 to 1993. *J Virol* 77(15):8366–8377.
6. Kew OM, et al. (2004) Policy and Practice Circulating vaccine-derived polioviruses: current state of knowledge. *Bull World Health Organ* 82(1).
7. World Health Organization (2016) Rationale and timelines for OPV withdrawal. Available at: https://web.archive.org/web/20160802182547/http://www.who.int/immunization/diseases/poliomyelitis/endgame_objective2/oral_polio_vaccine/planning/en/ [Accessed August 2, 2016].
8. Koopman J S, et al. Dynamics Affecting the Risk of Silent Circulation When Oral Polio Vaccination Is Stopped. doi:10.1101/058099.
9. Thompson KM, Duintjer Tebbens RJ Modeling the Dynamics of Oral Poliovirus Vaccine Cessation. doi:10.1093/infdis/jit845.
10. Korotkova EA, et al. (2003) Retrospective Analysis of a Local Cessation of Vaccination against Poliomyelitis: a Possible Scenario for the Future. *J Virol* 77(23):12460–12465.
11. Shimizu H, et al. (2004) Circulation of Type 1 Vaccine-Derived Poliovirus in the Philippines in 2001. *J Virol* 78(24):13512–13521.
12. Martín J, Ferguson GL, Wood DJ, Minor PD (2000) The Vaccine Origin of the 1968 Epidemic of Type 3 Poliomyelitis in Poland. *Virology* 278(1):42–49.
13. Centers for Disease Control and Prevention (2007) Update on Vaccine-Derived Polioviruses - Worldwide, January 2006-August 2007. *MMWR* 56(38):996–1001.
14. Klein DJ, et al. (2014) The Separatrix Algorithm for Synthesis and Analysis of Stochastic Simulations with Applications in Disease Modeling. *PLoS One* 9(7):e103467.
15. Beale AJ (1991) Efficacy and safety of oral poliovirus vaccine and inactivated poliovirus vaccine. *Pediatr Infect Dis J* 10(12):970–2.

16. Stickle G (1964) Observed and Expected Poliomyelitis in the United States, 1958-1961. *Am J Public Health* 54(8):1222–1229.

17. Asturias EJ, et al. (2016) Humoral and intestinal immunity induced by new schedules of bivalent oral poliovirus vaccine and one or two doses of inactivated poliovirus vaccine in Latin American infants: an open-label randomised controlled trial. *Lancet* 388(10040):158–169.

18. O'Ryan M, et al. (2015) Inactivated poliovirus vaccine given alone or in a sequential schedule with bivalent oral poliovirus vaccine in Chilean infants: a randomised, controlled, open-label, phase 4, non-inferiority study. *Lancet Infect Dis* 15(11):1273–82.

19. Ghendon Y, Sanakoyeva I (1961) Comparison of the resistance of the intestinal tract to poliomyelitis virus (Sabin's strains) in persons after naturally and experimentally acquired immunity. *Acta Virol*. Available at: https://scholar.google.com/scholar?q=+Acta+Virol+1961+%3B5%3A265-73&btnG=&hl=en&as_sdt=0%2C48#0 [Accessed September 17, 2015].

20. Hird TR, Grassly NC (2012) Systematic review of mucosal immunity induced by oral and inactivated poliovirus vaccines against virus shedding following oral poliovirus challenge. *PLoS Pathog* 8(4):e1002599.

21. Wringe A, Fine PEM, Sutter RW, Kew OM (2008) Estimating the Extent of Vaccine-Derived Poliovirus Infection. *PLoS One* 3(10):e3433.

22. Wassilak S, et al. (2011) Outbreak of Type 2 Vaccine-Derived Poliovirus in Nigeria: Emergence and Widespread Circulation in an Underimmunized Population. *J Infect Dis* 203(7):898–909.

23. Global Polio Eradication Initiative (2016) Polio this week as of 17 August 2016. Available at: https://web.archive.org/web/20160818185304/http://www.polioeradication.org/dataandmonitoring/poliothisweek.aspx [Accessed August 18, 2016].

24. Global Polio Eradication Initiative (2016) Key Countries, Nigeria; June 20, 2016. Available at: https://web.archive.org/web/20160620214959/http://www.polioeradication.org/Keycountries/Nigeria%28cVDPV%29.aspx [Accessed January 1, 2016].

25. ECDC (2014) Monitoring current threats: ECDC Communicable... Available at: https://web.archive.org/web/20160810013610/http://ecdc.europa.eu/en/press/news/_layouts/forms/News_DispForm.aspx?List=8db7286c-fe2d-476c-9133-18ff4cb1b568&ID=1065 [Accessed August 9, 2016].

26. Dunn G, et al. (2015) Twenty-Eight Years of Poliovirus Replication in an Immunodeficient Individual: Impact on the Global Polio Eradication Initiative. *PLOS Pathog* 11(8):e1005114.

27. Bandyopadhyay AS, Garon J, Seib K, Orenstein WA (2015) Polio vaccination: past, present and future. *Future Microbiol* 10(5):791–808.

28. Macadam AJ, et al. (2006) Rational design of genetically stable, live-attenuated poliovirus vaccines of all three serotypes: relevance to poliomyelitis eradication. *J Virol* 80(17):8653–63.

29. Lauring AS, Jones JO, Andino R (2010) Rationalizing the development of live attenuated virus vaccines. *Nat Biotechnol* 28(6):573–9.

30. EMOD Documentation (2016) Available at:

http://idmod.org/idmdoc/#EMOD_top/GettingStartedTOC.htm [Accessed August 2, 2016].

31. POLIS: The polio information system Available at: https://extranet.who.int/polis/Search [Accessed August 2, 2016].

32. John J, et al. (2014) Effect of a single inactivated poliovirus vaccine dose on intestinal immunity against poliovirus in children previously given oral vaccine: an open-label, randomised controlled trial. *Lancet (London, England)* 384(9953):1505–12.

33. Jafari H, et al. (2014) Polio eradication. Efficacy of inactivated poliovirus vaccine in India. *Science* 345(6199):922–5.

34. World Health Organization Media Centre (2016) Government of Nigeria reports 2 wild polio cases, first since July 2014. *WHO*. Available at: https://web.archive.org/web/20160818185430/http://www.who.int/mediacentre/news/releases/2016/nigeria-polio/en/ [Accessed August 18, 2016].

Figure Legends

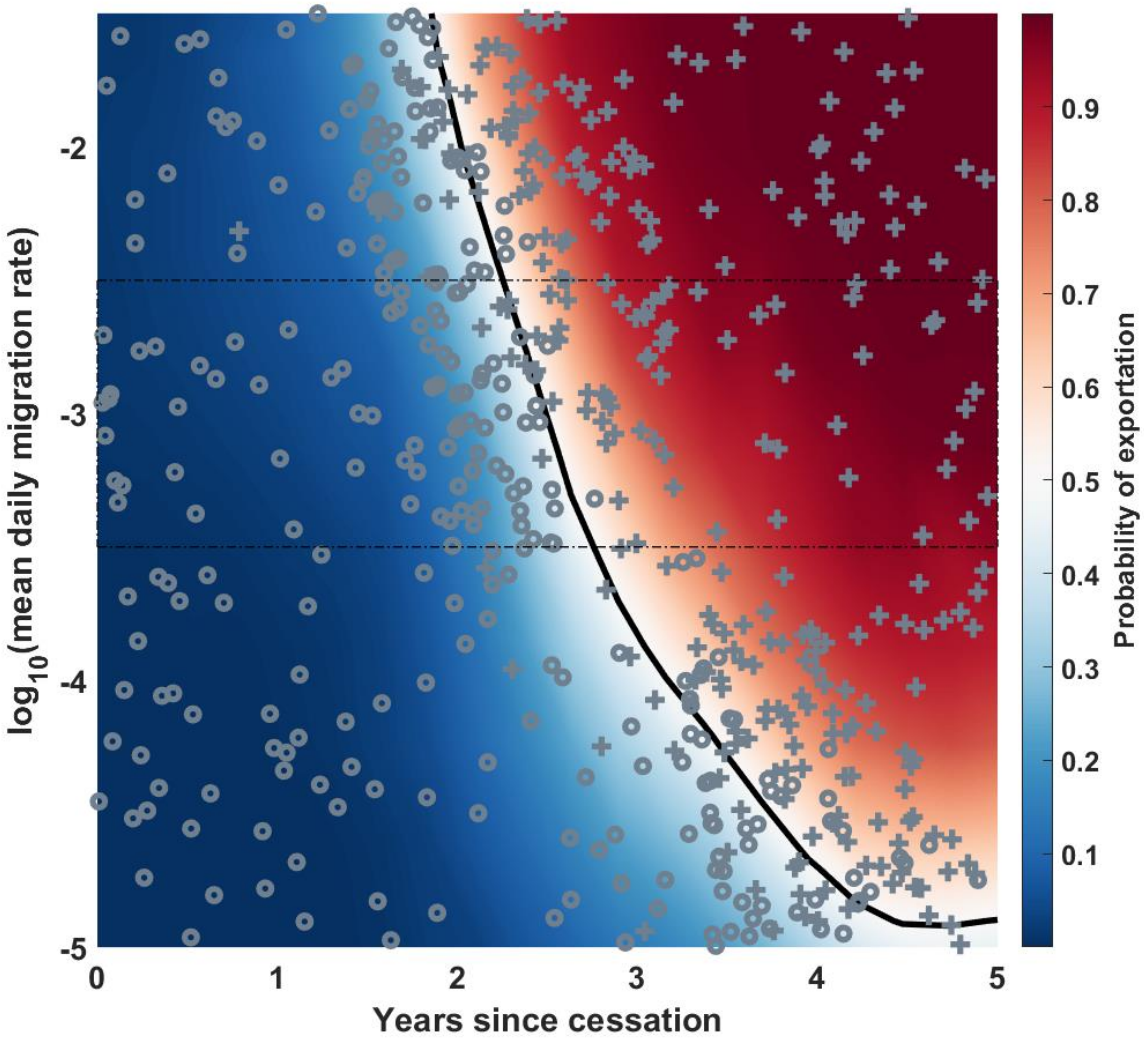

Figure 1: Example output from a single Separatrix scenario, with R_{0f} = 2.0, f = 0.5, λ= 60 days, N_{IPV}= 1, c= 1. The colored surface represents the probability that the OPV2 used in outbreak response continues to circulate, outside of the response region, 9 months after the final response campaign. The black solid line represents the parameter contour along which this probability is 50%. Gray crosses represent simulations in which this exportation and survival outcome occurs, and gray circles represent those in which it does not. The thin black dashed box indicates migration rates that are preferred by a calibration to a single travelling WPV1 outbreak in the region, in 2008. The distribution of simulated points illustrates the behavior of the algorithm; the first round of the separatrix algorithm broadly explores the space, and the second concentrates simulations around the contour of interest.

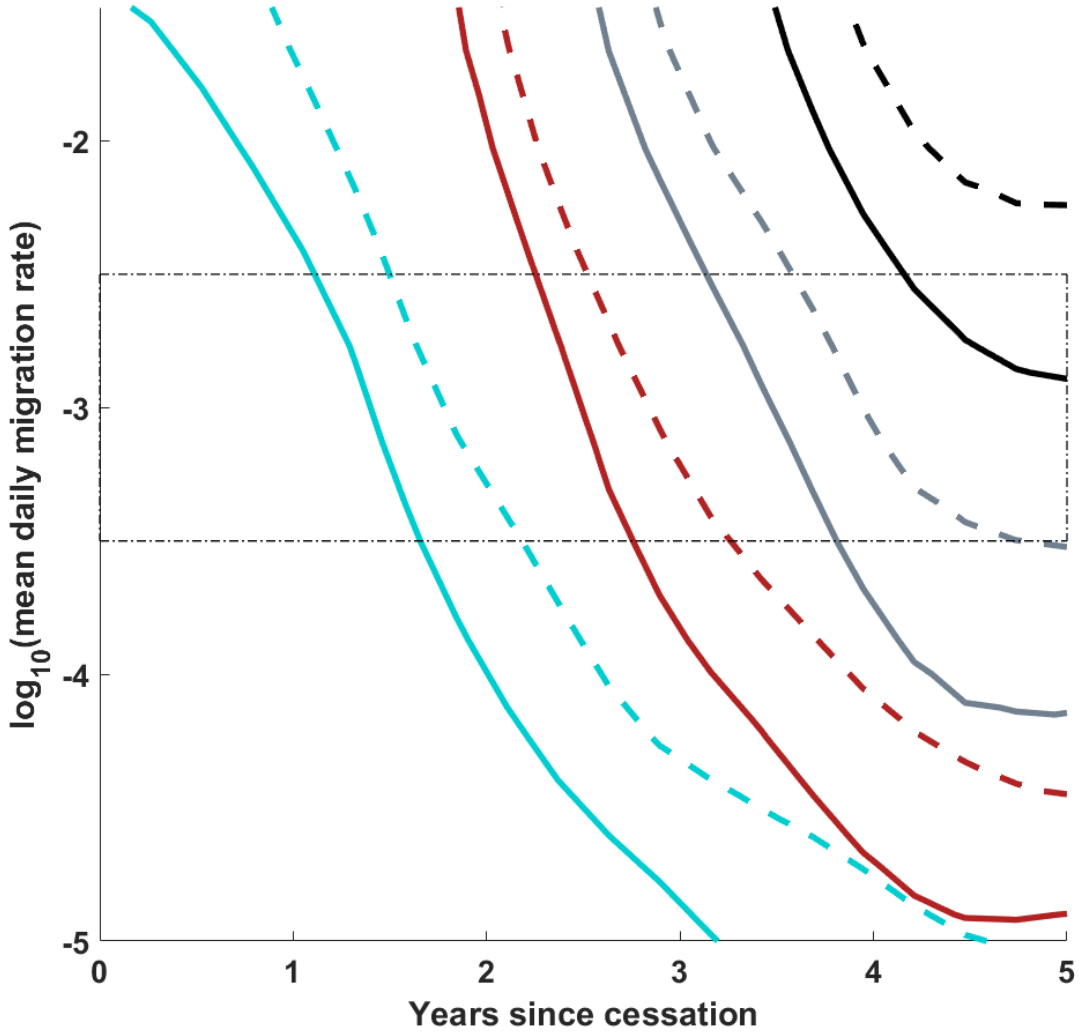

Figure 2: Position of the 50% separatrix line as the R_0 profile of OPV2 varies, at constant λ= 60 days, N_{IPV}= 1, c= 1. The solid and dashed lines respectively indicate f=0.5 and f=0.25, while the cyan, red, grey, and black respectively indicate R_{0f} values of 3, 2, 1.5, and 1.2. The thin black dashed box indicates migration rates that are preferred by a calibration to a single travelling WPV1 outbreak in the region, in 2008. The final R_0 is observed to have the dominant effect, with the risk at a given time point and migration rate decreasing with R_{0f} as expected. The initial R_0 multiplier has a comparatively small effect, but a lower initial R_0 does also mitigate the survival risk.

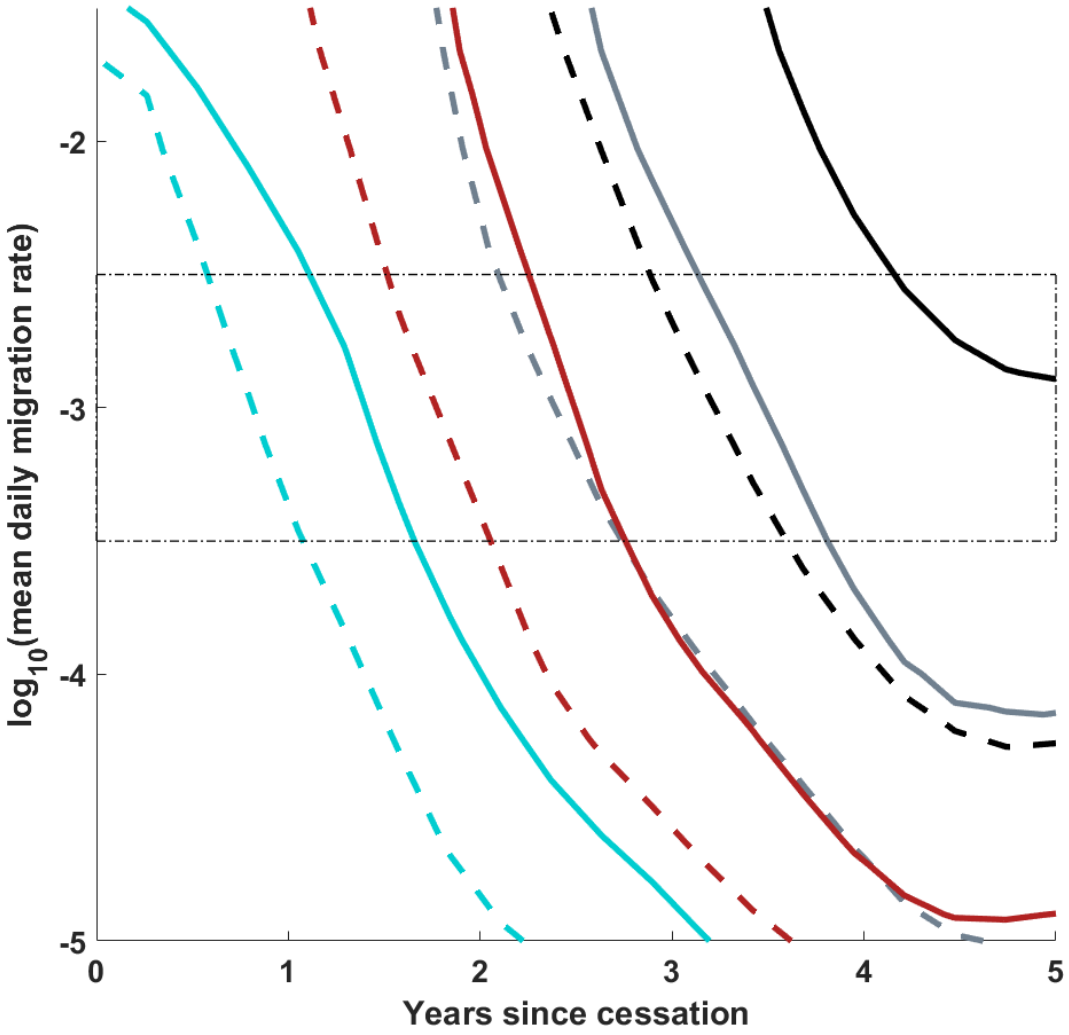

Figure 3: Position of the 50% separatrix line as number of IPV doses in routine immunization varies, at constant λ= 60 days, f = 0.5, c= 1. The dashed and solid lines respectively indicate N_{IPV} = 0 or 1, and the cyan, red, grey, and black respectively indicate R_{0f} values of 3, 2, 1.5, and 1.2. The thin black dashed box indicates migration rates that are preferred by a calibration to a single travelling WPV1 outbreak in the region, in 2008. Under the assumptions made in this model regarding the population-level effects of IPV dosing, an additional dose of IPV in routine immunization in the cohort born after cessation provides a strong mitigating effect on the risk of OPV2 survival and circulation at low R_0; the mitigating effect declines as the R_0 of the reverted virus increases.

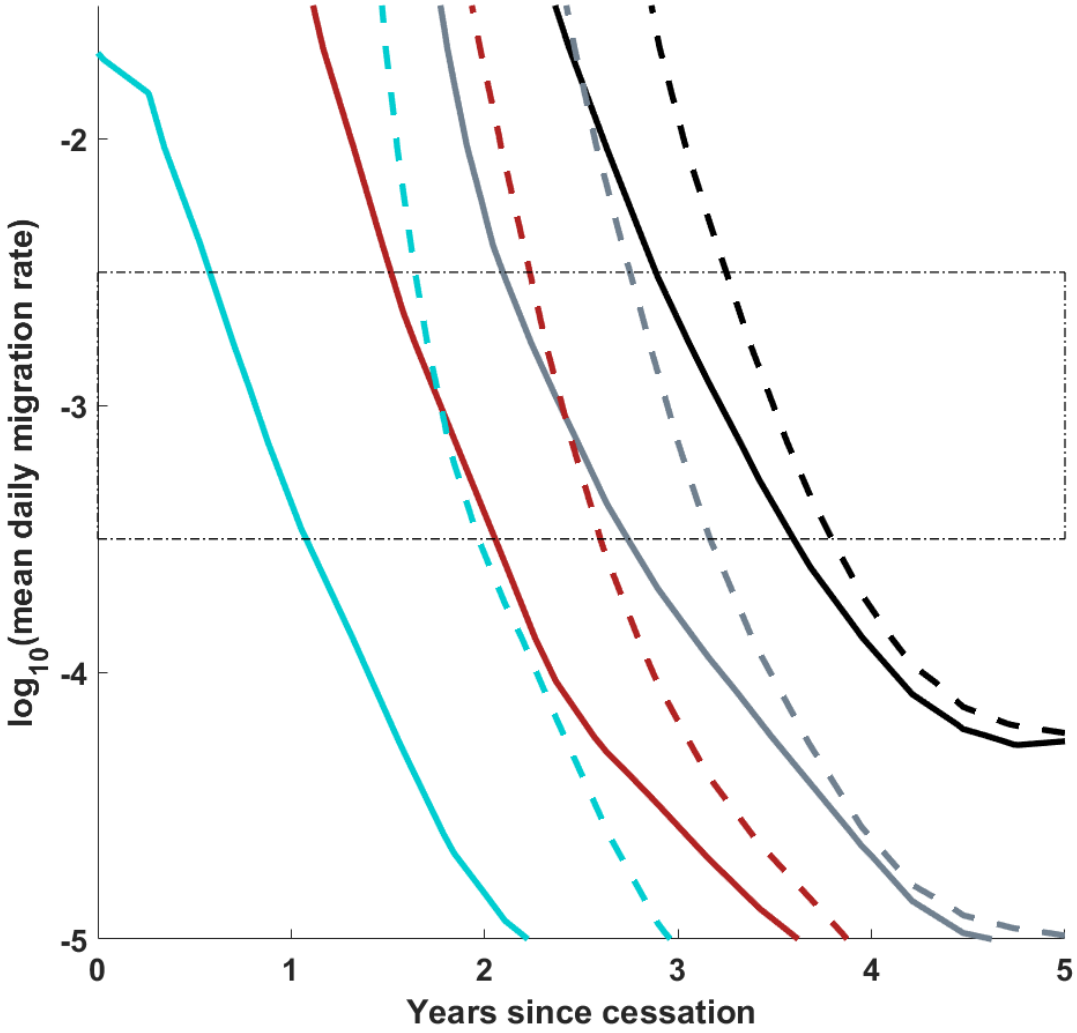

Figure 4: Dependence of the position of the 50% separatrix line on immunity levels in the cohort of children born before cessation: 100% immunity (dashed lines) vs. immunity induced by 3 rounds of OPV at 80% coverage, 50% take (solid lines). All lines at constant f=0.5, N_{IPV}= 1, c= 1, λ= 60 days. The cyan, red, grey, and black respectively indicate R_{0f} values of 3, 2, 1.5, and 1.2. The final R_0 is observed to have the dominant effect. The thin black dashed box indicates migration rates that are preferred by a calibration to a single travelling WPV1 outbreak in the region, in 2008. The effect of increasing immunity in the older cohort is largest at higher R_0, as higher R_0 facilitates more transmission through partially immune older children. However, the additional protection is somewhat modest (considering the extreme assumption of perfect immunity in all children born pre-cessation), indicating that the cohort of children born post-cessation rapidly becomes a dominant contributor to OPV2 transmission in this model.

Supplemental Information

Model Specification

The EMOD model is an individual-based stochastic model of disease transmission, with support for campaign implementation, heterogeneous transmission, and spatially segregated populations coupled by individual-level migration; the software also includes sub-packages implementing "generic", vector-borne, water-borne, airborne, and sexual disease transmission. The EMOD software is available for download at http://idmod.org/idmdoc/#EMOD/EMODBuildAndRegression/BuildingEMODTOC.htm. The model presented in this manuscript was developed within the EMOD "generic" simulation framework, implementing a discrete-time, individual-based form of a susceptible-exposed-infectious-susceptible model. Below, we review the adjustments to a simple SEIS model that were implemented in this model to reflect polio immunology and specify the model in terms of the individual-level state transition dynamics.

Individuals in the model exist in susceptible, exposed, and infectious states, with individuals returning to the susceptible state immediately upon clearance of an infection. However, infections with wild or Sabin-strain attenuated poliovirus, as well as vaccination with the inactivated polio vaccine, are known to confer partial immunity to individuals. Immunity in this model is characterized by two individual-level properties: acquisition-moderating immunity (α), which modulates the probability of infection given exposure to infectivity, and applies in the susceptible state; and transmission-moderating immunity (τ), which reduces the infectivity of an infectious individual. Both α and τ are defined on [0, 1], and are defined such that a completely naïve individual has both properties equal to 1. At α=0, an individual cannot be infected by any amount of exposure; at τ=0, an individual who becomes infected will not shed.

The parameters governing individual immunity are updated upon clearance of OPV infection or successful IPV vaccination. In the event of multiple vaccinations or infections, the α and τ parameters stack multiplicatively; these parameters thus aim to model a per-infection effect on acquisition- and transmission-modulating immunity. IPV vaccination behaves similarly, with per-dose effects on the two immunity channels, but IPV can provide two sets of effects; for individuals without a history of OPV infection, an IPV vaccination provides an individual with a small priming effect in each immunity channel, but for individuals with a history of OPV infection, IPV provides a larger boosting effect on immunity. As noted in the main text, current support for an incremental effect of additional IPV doses on the mucosal immunity of bOPV-exposed, OPV2-naïve children is not immediately apparent from the published literature. One recent study supports a dose-dependent effect while another finds no difference, though the two studies are in different settings and use different schedules.[1,2] This model does in fact implement a dose-dependent response, as it is simpler to implement and it should not affect the results - only a single dose of IPV in RI is modeled and compared against zero doses. A small subset of children in the model may receive the RI IPV, be missed by the subsequent OPV campaigns, but receive a second dose of IPV in outbreak response; this cohort is sufficiently small that its effects are overwhelmed by the uncertainties in other model features (Sabin 2 R_0, overall demographics of immunity, migration rates and connections).

The infectious and incubation periods (γ and σ, respectively) were modeled using constant times spent in a compartment, rather than the exponential distribution implied by the rate parameters in a standard

SEIS model, changing the parameters from rates to delays in the equations. The mortality rate ν is implemented as a function of age ν(*a*), with values obtained from DHS[3]. The model tracks only 0-5 year olds, as ~98% of all cVDPV2 paralysis cases in the AFRO region have arisen in this cohort.[4] As the case load is concentrated in this age group, the authors think it likely that virus transmission is also highly concentrated in this cohort. To the extent that silent circulation occurs in older cohorts, for the purposes of modeling, outbound and inbound transmission from the observable cohort to the silent cohort can be reduced to an effective transmission rate within the observable cohort. The effective birth rate is adjusted to produce a population growth rate of 2.8% per year[3].

The model includes a linear rising exposure to infectiousness with age. This term is based on previous work modeling WPV1 paralysis cases in Kano state, Nigeria (reference), where the number of paralysis cases peaked at 2 years of age, and the age distribution of cVDPV2 cases in AFRO exhibits a similar shape. This apparent protection lasts too long to be solely the effect of maternal antibodies, and so this rising susceptibility was developed to incorporate the effects of both maternal antibodies and reduced overall mixing with older children. Individual susceptibility vs. age is governed by the following equation:

$$\alpha(a) = \begin{cases} 0 & , f_0 + f_1 a \leq 0 \\ f_0 + f_1 a & , 0 < f_0 + f_1 a < 1 \\ 1 & , f_0 + f_1 a \geq 1 \end{cases} \quad (1)$$

Secondary infections arising from individual campaigns are not separately tracked, preventing the tracking of separate VDPV lineages undergoing independent reversion. Rather, infectivity is described as a function of time, held constant through the initial campaigns in the outbreak response and beginning to rise after the final campaign:

$$\beta(t) = \begin{cases} g\beta_f & , t < t_d \\ \beta_f * \left(1 - (1-g)e^{\frac{t-t_d}{\lambda}}\right) & , t \geq t_d \end{cases} \quad (2)$$

Individuals of any disease state and age migrate between metapopulations (nodes), which represent AdminL1 (provinces) of 16 West African countries (Senegal, Mauritania, Sierra Leone, Guinea, Liberia, Cote d'Ivoire, Mali, Burkina Faso, Ghana, Togo, Benin, Niger, Nigeria, Cameroon, Chad, Central African Republic). The infection process in a given node and at a given timestep is governed by individuals in that node at that timestep only. Individuals migrate between nodes (from a home node *i* to destination node *j*) with relative destination node rates according to a gravity-like model of migration; migration is modeled as one-day round-trips to prevent unrealistic population accumulation in the largest nodes.

$$M_{ij} = \kappa \frac{p_j}{d_{ij}^c} \quad (3)$$

Where *c* = 1 or 2 for the scenarios tested.

Individual-level transitions

With all of this in hand, individuals can be specified by a state space of {disease state *X*, age *a*, time in disease state t_X, home node *i*, current node *j,* acquisition-modulating immunity α, transmission-modulating immunity τ}. The absolute simulation time *t* also plays a role due to immunization campaigns on specific dates and seasonal dynamics; this simulation state variable is shared by all individuals.

Disease state transitions, vital dynamic transitions, and migration transitions are treated independently from one another, simplifying the specification of the transition space. The individual-level state transitions are presented below in the order in which they are processed in simulation.

For the sake of readability, elements of the full state $\{X, a, t_X, i, j, \alpha, \tau\}$ that do not change in a given transition will be suppressed. *S, E,* and *I* without subscripts will indicate an individual's disease state, and with subscripts *j* will indicate the total population in state *X* in node *j*. N_j indicates the total population of node *j*.

The first transition in a given timestep is aging:

$$p(\{a, t_X\} \rightarrow \{a + \Delta, t_X + \Delta\}) = 1 \quad (4)$$

Next, OPV and IPV immunization interventions are processed:

IPV immunization:	$p(\{\alpha, \tau\} \rightarrow \{\alpha^*, \tau^*\}) = C_{kj}\delta(t - t_k)$	(5)
OPV immunization:	$p(\{S, t_S\} \rightarrow \{E, 0\}) = \tau C_{kj}\delta(t - t_k)$	(6)

Where C_{kj} indicates the effective coverage of the campaign *k* in node *j* (accounting for the effective take of OPV), δ is the Kronecker delta function, and t_k is the date of campaign *k*.

The infectious dynamics follow:

The total infectiousness in node *j* is given by the sum over infectious individuals *k* in node *j:*

$$\beta_{tot,j} = \sum_{k=1}^{I_j} \tau_k * \beta \quad (7)$$

$p(\{S, t_S\} \rightarrow \{E, 0\}) = 1 - exp\left(-\frac{\Delta\beta_{tot,j} * \alpha}{N_j(t)}\right)$	(8)
$p(\{E, t_E\} \rightarrow \{I, 0\}) = \delta(t_E - \sigma)$	(9)
$p(\{I, t_I, \alpha, \tau\} \rightarrow \{S, 0, \alpha^*, \tau^*\}) = \delta(t_I - \gamma)$	(10)

Deaths are processed next:

$p(\{X, a, t_X, i, j, \alpha, \tau\} \rightarrow \{\emptyset\}) = \Delta\nu(a)$	(11)

Followed by migration – again, outbound migration follows the rates in Eq. **Error! Reference source not found.**, and homebound migration always takes place the following timestep:

$p(\{i, i\} \rightarrow \{i, j \neq i\}) = \Delta M_{ij}$	(12)
$p(\{i, j \neq i\} \rightarrow \{i, i\}) = 1$	(13)

Finally, new births are processed:

$N(\{\emptyset\} \rightarrow \{S, 0, 0, i, i, 0, 0\}) = Poiss(\Delta\mu N_i(t))$	(14)

Equations **Error! Reference source not found.** combine to specify the agent-based model as implemented. This specification can also be converted into a set of stochastic difference equations; the

resulting equations are rather unwieldy and somewhat difficult to read, limiting how informative they are to the reader. The relevant model parameters are summarized in Table 2.

Parameter description (symbol)	Value(s)	Relevant effect or equation	Comparison references
OPV transmission modifier (τ_{OPV})	0.9	Upon clearance of OPV infection or IPV immunization in OPV-exposed individuals: $\tau \rightarrow \tau * (1 - \tau_{OPV})$	[5–7]
OPV acquisition modifier (α_{OPV})	0.6	Upon clearance of OPV infection or IPV immunization in OPV-exposed individuals: $\alpha \rightarrow \alpha * (1 - \alpha_{OPV})$	[5–7]
IPV transmission modifier (τ_{IPV})	0.1	Upon IPV immunization in OPV-naïve individuals: $\tau \rightarrow \tau * (1 - \tau_{IPV})$	[5–7]
IPV acquisition modifier (α_{IPV})	0.1	Upon IPV immunization in OPV-naïve individuals: $\alpha \rightarrow \alpha * (1 - \alpha_{IPV})$	[5–7]
Age-dependent susceptibility intercept (f_0)	0.0	$\alpha(a) = (f_0 + f_1 a)$	
Age-dependent susceptibility slope (f_1)	0.5	$\alpha(a) = (f_0 + f_1 a)$	
Migration rate scalar (κ)	Varied in separatrix	$M_{ij} = \kappa \frac{p_j}{d_{ij}^c}$	[8]
Migration rate distance dependence (c)	{1, 2}	$M_{ij} = \kappa \frac{p_j}{d_{ij}^c}$	[8]
Duration of exposed state (σ)	3	$p(\{E, t_E\} \rightarrow \{I, 0\}) = \delta(t_E - \sigma)$	[5,6]
Duration of infectious state (γ)	27	$p(\{I, t_I, \alpha, \tau\} \rightarrow \{S, 0, \alpha^*, \tau^*\}) = \delta(t_I - \gamma)$	[5,6]
Initial infectiousness of Sabin 2 relative to fully-reverted (f)	{0.25, 0.5}	$\beta(t) = \begin{cases} f\beta_f & , t < t_d \\ \beta_f * \left(1 - (1-f)e^{\frac{t-t_d}{\lambda}}\right) & , t \geq t_d \end{cases}$	[6]
Final R_0 of reverted Sabin 2	{1.2, 1.5, 2, 3}	$R_0 = \frac{\beta_f * \gamma}{\int \alpha(a) * f(a) da}$ Denominator indicates correction for age-dependent susceptibility, with $\alpha(a)$ defined as in (1) and $f(a)$ the population age distribution.	
Delay before Sabin reversion (t_d)	86 (time of final outbreak response campaign)	$\beta(t) = \begin{cases} g\beta_f & , t < t_d \\ \beta_f * \left(1 - (1-g)e^{\frac{t-t_d}{\lambda}}\right) & , t \geq t_d \end{cases}$	
Timescale of Sabin reversion (λ)	{60, 150}	$\beta(t) = \begin{cases} g\beta_f & , t < t_d \\ \beta_f * \left(1 - (1-g)e^{\frac{t-t_d}{\lambda}}\right) & , t \geq t_d \end{cases}$	[9]

Table 2: Description of all model parameters relevant to the study

Calibration

In 2008, a seasonal peak in endemic transmission in Nigeria apparently seeded outbreaks that propagated over the following two years throughout the West African countries modeled in this work. Comparing this historical outbreak with the behavior of modeled outbreaks allows for qualitative bounds to be placed on the magnitude of migration rates in the model. Figure 5 presents this historical outbreak, with countries placed into a rough ordering from northwest at the top to southeast at the bottom, producing a striking traveling epidemic pattern.

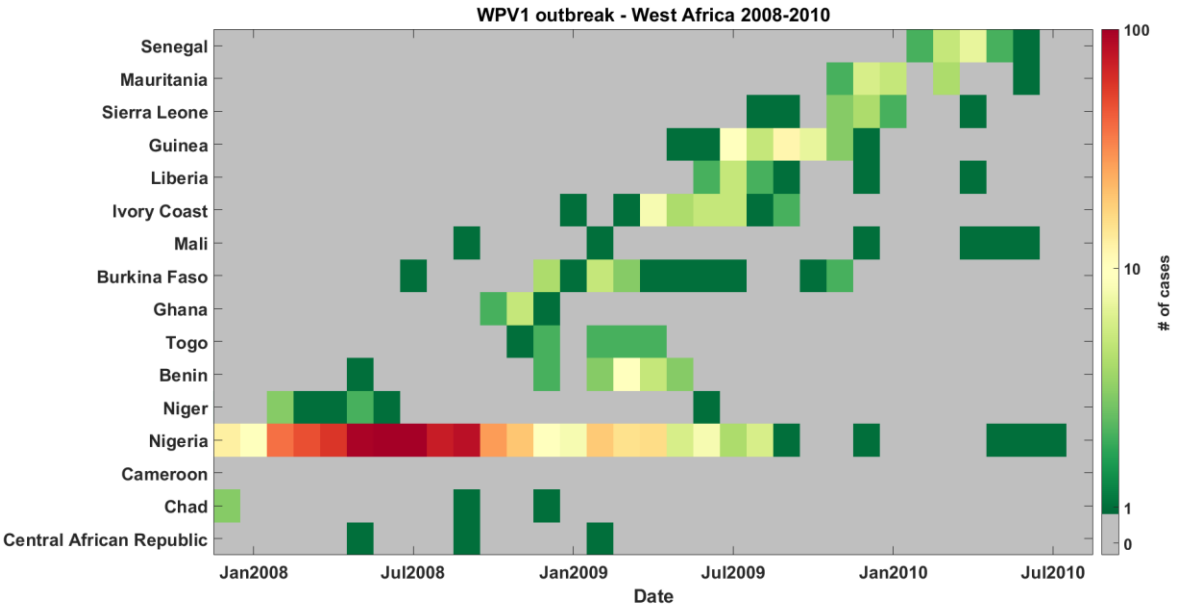

Figure 5: Wild Poliovirus Type 1 outbreak in West Africa, 2008-2010. Countries are roughly ordered northwest to southeast from top to bottom.

Calibrating the properties of the modeled migration network to this past poliovirus outbreak presents inherent difficulties – due to the case-to-infection ratio, the spread of infection is poorly sampled; disease propagation on the network is stochastic, and only a single observation of propagation on the network is observed; and the propagation process depends not only on the structure of the migration network, but also on the uncertain transmissibility and immunity conditions in the nodes of the network. For these reasons, a detailed calibration of the migration models to the full spatial infection traces is not attempted. Rather, calibration qualitatively targets the temporal behavior of the outbreak, seeking to minimize the differences between a "case-weighted time" in each country from data (Eq. 15**Error! Reference source not found.**) and "incidence-weighted time" from simulation in each country (Eq. 16). The relative amplitudes of the outbreaks in different countries are not targeted as part of the calibration.

$$\overline{t_{j,data}} = \frac{\left(\sum_t t * C_{j,t}\right)}{\sum_t\left(C_{j,t}\right)}$$	**(15)**
$$\overline{t_{j,sim}} = \frac{\left(\sum_t t * I_{j,t}\right)}{\sum_t\left(I_{j,t}\right)}$$	**(16)**
$$\sigma = \sqrt{\sum_j\left(\overline{t_{j,data}} - \overline{t_{j,sim}}\right)^2}$$	**(17)**

With t stepping in 30-day increments beginning on Jan 1, 2008; $C_{j,t}$ indicating the number of cases in country j during time bin t, and $I_{j,t}$ indicating the number of infections in country j during time bin t. As the exact peak of the Nigeria outbreak may shift from simulation to simulation, $\overline{t_{j,sim}}$ is defined relative to that peak in each simulation. The calibration aims to minimize the term σ defined in Eq. 17 above (in practice, it actually aims to maximize $-log10(\sigma)$).

Incremental Mixture Importance Sampling (IMIS) is used to sample and re-sample a 2D parameter space of R_0 and overall migration rate.[10] IMIS was designed to work with deterministic models and proportionally sample a true posterior density based on an appropriately-defined likelihood function. However, the author has found it effective as a means of maximizing and mapping the surface of an objective function (not necessarily likelihoods) applied to a stochastic model, so long as the stochastic variance in the objective function at a single point is outweighed by the "parameter-based" variation throughout the calibration space - in some sense, as long the objective surface is "smooth", or has a high signal-to-noise. Additionally, a code base for interfacing IMIS directly to IDM's computational cluster already exists from previous work.

The model utilized in calibration is not strictly equivalent to that used in the investigations of post-cessation outbreak behavior. The immunity levels in each province are not set equal to each other, but are rather derived from vaccine dose histories reported by acute flaccid paralysis cases during the time period in question.[11] Partial immunity is also not treated in the calibration version of the model; transmission takes place only through fully susceptible children. Simulations begin in January 2008, with an outbreak seeded in Nigeria, and run through June 2013 (though the comparison only considers times through July 2010).

Figure 6 presents the results of the calibration; points in the 2D space represent a single sampled pair of infectivity and κ values, and the color indicating $-log10(\sigma)$. A broad maximum is apparent around mean migration rates from approximately -3.5 to -2.5 (in log-10 units), representing the preferred region outlined in the figures in the main text; this corresponds to the average child traveling outside of their home state approximately once per year to once per decade. Figure 7 presents the infection traces from two representative simulations in the preferred region under the actual outbreak. Above this range of migration rates, transmission across the region becomes increasingly synchronous, qualitatively ruling out these values as realistic; an example is shown in Figure 8. Below this preferred region, the metapopulations become more disconnected and transmission fails to export broadly across the network; an example is shown in Figure 9.

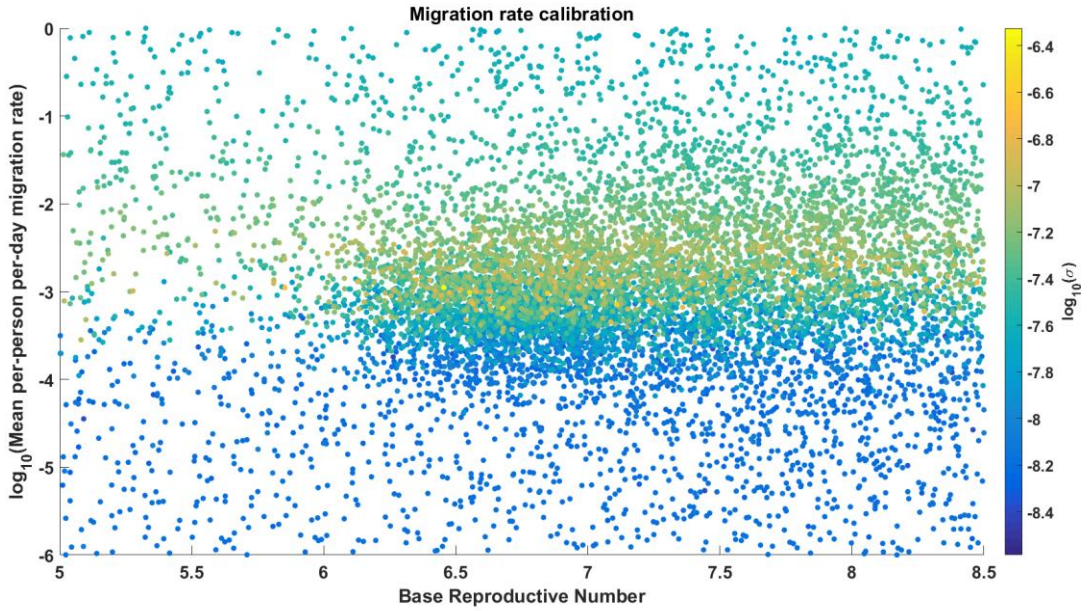

Figure 6: Results of calibration of migration rates. The x and y- axes represent the infectivity and mean migration rate, respectively, with color indicating the value of the objective function defined in Eqs (15-17). The results indicate a broad maximum around mean migration rates from roughly -3.5 to -2.5 (in log10 units), i.e., the average child leaving their home state approximately once per year to once per decade.

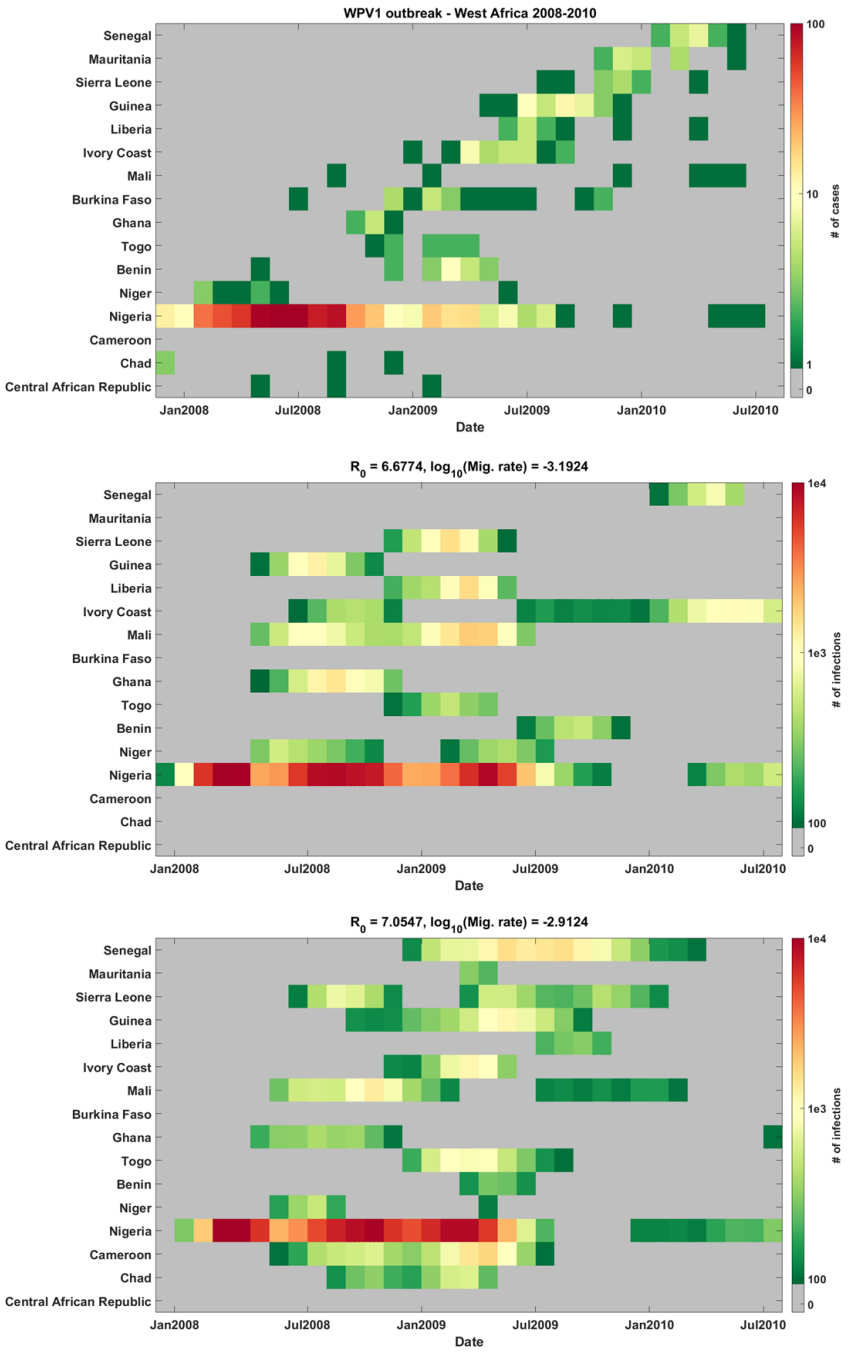

Figure 7: Top: WPV1 outbreak in West Africa, 2008-2010, representing the calibration target for this exercise. Middle and bottom: Two example simulation outputs from the preferred region of parameter space.

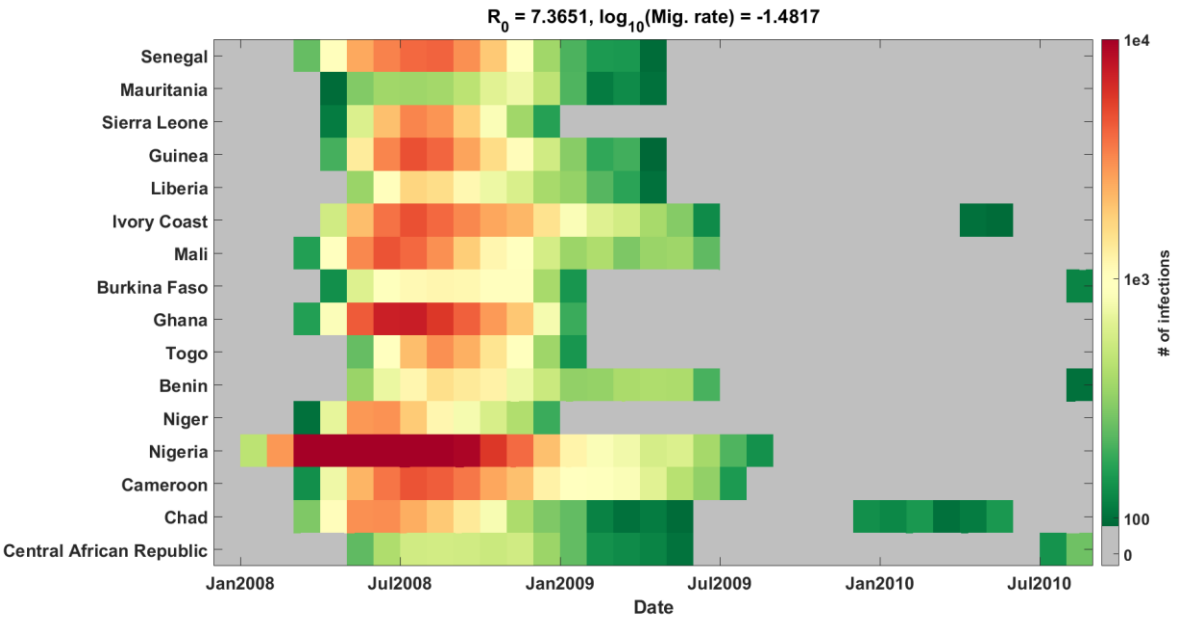

Figure 8: Example simulation output with migration rate set above the preferred range from calibration. As can be seen, transmission across the region is essentially synchronous, in contrast to the travelling outbreak actually observed.

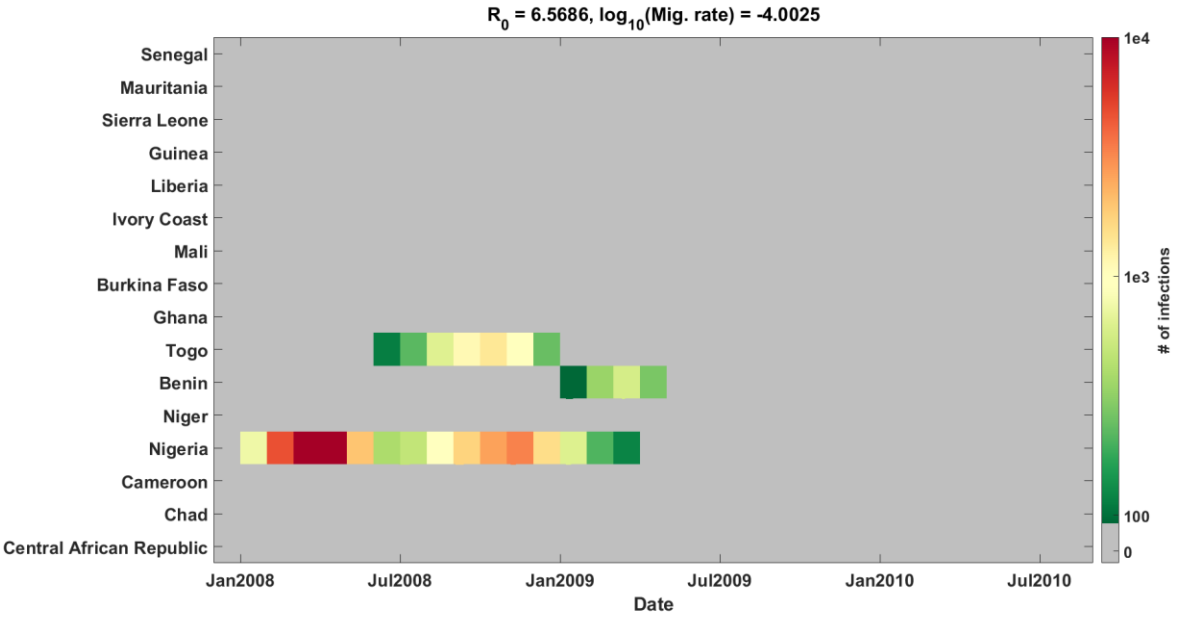

Figure 9: Example simulation output with migration rate set below the preferred range from calibration. In this case, transmission fails to export broadly across the region (though one or two exportations are not uncommon to observe), in contrast to the travelling outbreak observed in 2008.

While the simulations investigating the risk of Sabin 2 use post-cessation are allowed to explore a wide range of migration rates, this calibration allows for the identification of a preferred region of migration space, aiding interpretability of the results.

Additional figures

The simulation metapopulations are generated by applying WHO shapefiles from POLIS to population maps of Africa obtained from the Worldpop collaboration.[4,12] Figure 10 illustrates the population map (color) and country/province boundaries (thick/thin black solid lines) that were used. The total size of a given metapopulation is the aggregated sum of the per-pixel population map within the boundaries, and each population is placed at the population-weighted centroid of the province (for purposes of computing distances between metapopulations in the gravity model of migration).

Changing the distance-dependence in the gravity model of migration is found to have a negligible effect on the position of the separatrix line, with an inverse-linear distance-dependence (c=1, relatively higher migration rates to provinces of highest population) producing very slightly more risk than an inverse-square dependence (c=2, relatively higher migration rates to nearest neighbor provinces). Figure 11 presents the results of this comparison.

Figure 12 shows that increasing the timescale of Sabin 2 reversion from λ= 60 days to λ= 150 days provides a moderate mitigation of the survival risk, similar to the effect of changing f from 0.5 to 0.25 and small compared to the effects of changing R_{0f} or N_{IPV}. However, at the lower values of R_{0f} tested in these scenarios, a longer reversion timescale can have substantial impact, as the effective reproductive number of the circulating Sabin 2 remains well below 1 for multiple generations of infection after the campaigns.

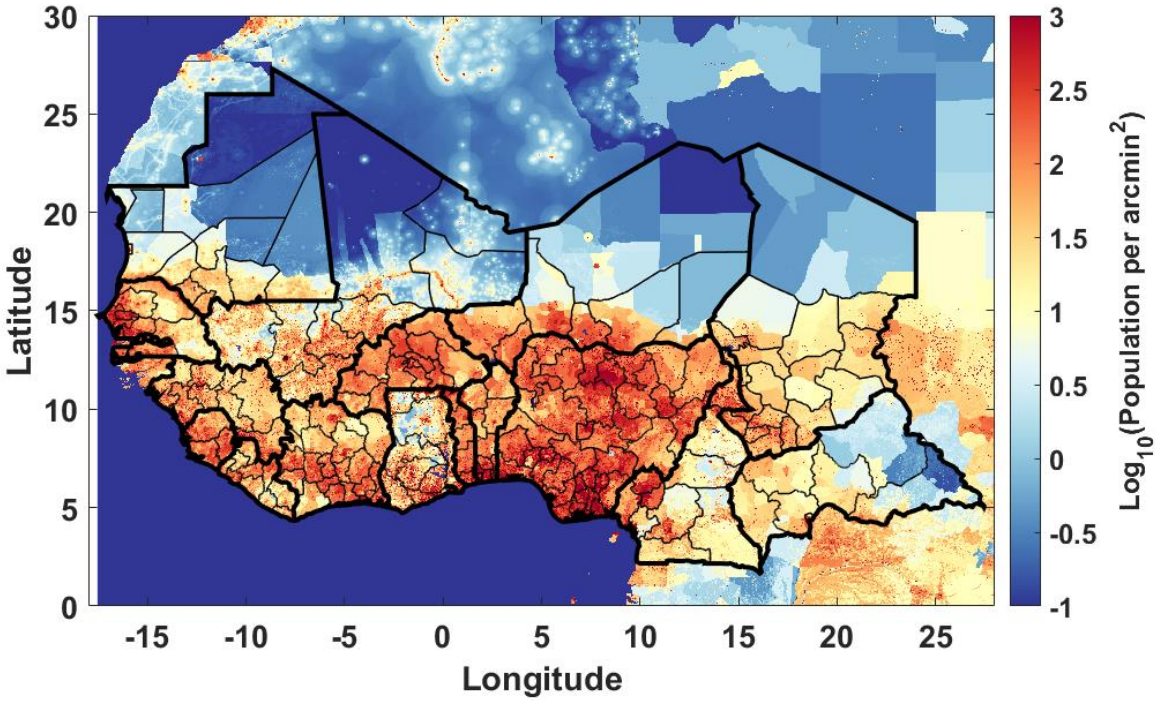

Figure 10: Population map (from Worldpop) and country/province boundaries (thick/thin solid black lines, from POLIS) used to generate the metapopulations for the simulation.[4,12] The boundaries and names shown and the designations used in the maps in the supplement of this document do not imply the expression of any opinion whatsoever on the part of the World Health Organization concerning the legal status of any country, territory, city, or area or of its authorities, or concerning the delimitation of its frontiers or boundaries.

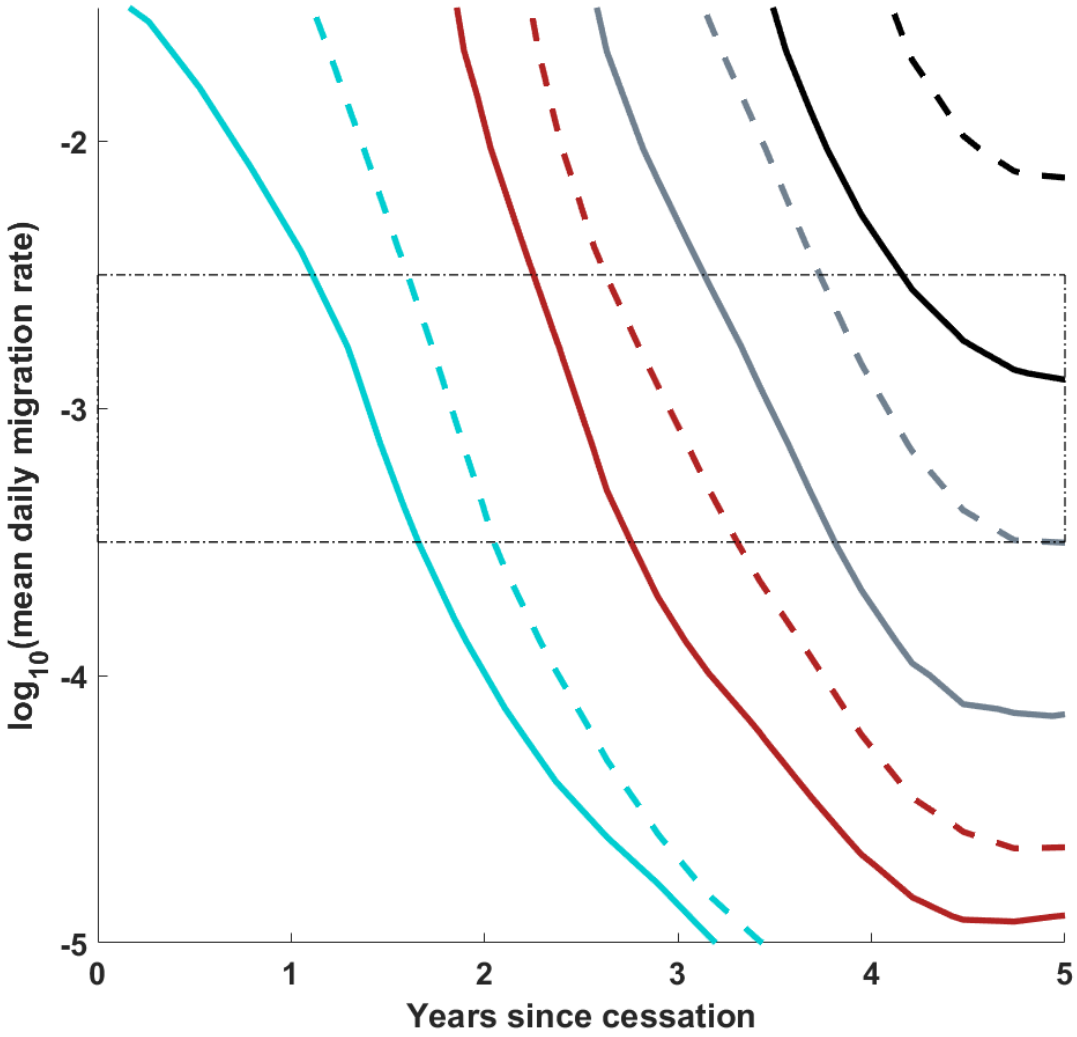

Figure 11: Position of the 50% separatrix line as the distance dependence in the gravity model of migration varies, at constant λ= 60 days, N_{IPV}= 1, c= 1. The solid and dashed lines respectively indicate c = 1 and c = 2, while the cyan, red, grey, and black respectively indicate R_{0f} values of 3, 2, 1.5, and 1.2. The relative distribution of migration rates in the network induces a negligible effect compared with the overall mean migration rate of individuals on the network to all possible destinations.

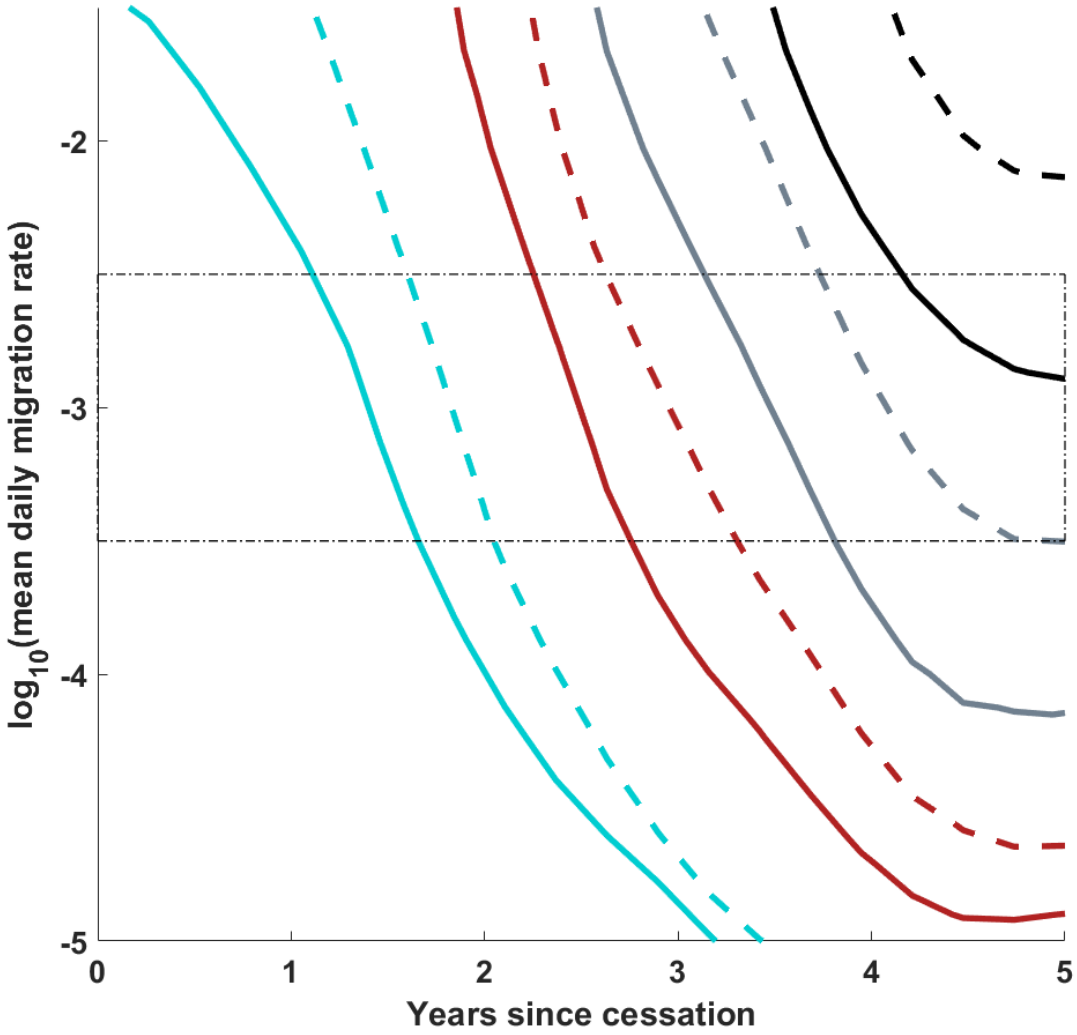

Figure 12: Position of the 50% separatrix line as the timescale of R_0 reversion varies, at constant f=0.5, N_{IPV}= 1, c= 1. The solid and dashed lines respectively indicate λ= 60 days and λ= 150 days, while the cyan, red, grey, and black respectively indicate R_{0f} values of 3, 2, 1.5, and 1.2. The final R_0 is observed to have the dominant effect. At the higher values of R_{0f}, changing the reversion timescale provides minimal mitigation of the Sabin 2 survival risk, but the effect grows at lower values of R_{0f}, as the effective reproductive rate of Sabin 2 remains below 1 for more transmission generations.

References

1 Asturias EJ, Bandyopadhyay AS, Self S, *et al.* Humoral and intestinal immunity induced by new schedules of bivalent oral poliovirus vaccine and one or two doses of inactivated poliovirus vaccine in Latin American infants: an open-label randomised controlled trial. *Lancet* 2016; **388**: 158–69.

2 O'Ryan M, Bandyopadhyay AS, Villena R, *et al.* Inactivated poliovirus vaccine given alone or in a sequential schedule with bivalent oral poliovirus vaccine in Chilean infants: a randomised,

controlled, open-label, phase 4, non-inferiority study. *Lancet Infect Dis* 2015; **15**: 1273–82.

3 National Population Commission - Federal Republic of Nigeria, ICF International. Nigeria Demographic and Health Survey, 2013 - Final Report. 2014.

4 POLIS: The polio information system. https://extranet.who.int/polis/Search (accessed Aug 2, 2016).

5 Behrend MR, Hu H, Nigmatulina KR, Eckhoff P. A quantitative survey of the literature on poliovirus infection and immunity. *Int J Infect Dis* 2014; **18**: 4–13.

6 Duintjer Tebbens RJ, Pallansch MA, Kalkowska DA, Wassilak SGF, Cochi SL, Thompson KM. Characterizing poliovirus transmission and evolution: insights from modeling experiences with wild and vaccine-related polioviruses. *Risk Anal* 2013; **33**: 703–49.

7 Hird TR, Grassly NC. Systematic review of mucosal immunity induced by oral and inactivated poliovirus vaccines against virus shedding following oral poliovirus challenge. *PLoS Pathog* 2012; **8**: e1002599.

8 Wesolowski A, Buckee CO, Pindolia DK, *et al.* The Use of Census Migration Data to Approximate Human Movement Patterns across Temporal Scales. *PLoS One* 2013; **8**: e52971.

9 Duintjer Tebbens RJ, Pallansch MA, Kim J-H, *et al.* Oral poliovirus vaccine evolution and insights relevant to modeling the risks of circulating vaccine-derived polioviruses (cVDPVs). *Risk Anal* 2013; **33**: 680–702.

10 Raftery AE, Bao L. Estimating and Projecting Trends in HIV/AIDS Generalized Epidemics Using Incremental Mixture Importance Sampling. *Biometrics* 2010; **66**: 1162–73.

11 Upfill-Brown AM, Lyons HM, Pate MA, *et al.* Predictive spatial risk model of poliovirus to aid prioritization and hasten eradication in Nigeria. *BMC Med* 2014; **12**: 92.

12 WorldPop Collaboration. Worldpop - Selected Data: Africa > Whole Continent > Population 2010. 2012. http://www.worldpop.org.uk/data/summary/?contselect=Africa&countselect=Whole+Continent&typeselect=Population+2010 (accessed Aug 24, 2016).